Aggregation Structure Development and Mechanical Properties of Biodegradable Poly(butylene succinate-*co*-terephthalate) Fibers

Shengli Luo,[1,2] Faxue Li,[1] Jianyong Yu,[3] Amin Cao[4]

[1]Key Laboratory of Textile Science and Technology, Ministry of Education, College of Textiles, Donghua University, Shanghai 201620, People's Republic of China
[2]Technology department, Guangzhou Fiber Product Testing Institute, Haizhu District, Guangzhou 510220, People's Republic of China
[3]Research Institute of Donghua University, Shanghai 200051, People's Republic of China
[4]Laboratory for Polymer Materials, Shanghai Institute of Organic Chemistry, Chinese Academy of Sciences, Shanghai 200032, People's Republic of China

ABSTRACT: Biodegradable poly(butylene succinate-*co*-terephthalate)(PBST) copolyester, with 70 mol % butylene terephthalate (BT), was melt-spun into fibers at various take-up velocities ranging from 2.0 to 4.0 km/min. The structure development and mechanical properties of the as-spun PBST fibers were intensively investigated via birefringence, wide angle X-ray diffraction (WAXD) measurement, tensile test, and cyclic stretch test. With increasing the take-up velocity, the initial tensile modulus and breaking strength of PBST fibers increased, while elongation at break decreased. These were attributed to the increasing degree of orientation and crystallinity, which were resulted from the elevating tension of spinning line at higher take-up velocity. To elucidate the effects of soft butylene succinate (BS) unit on the tensile and elastic properties of PBST fibers, poly(butylene terephthalate) (PBT) fibers were adopted as a comparison sample. The results showed that the combination of soft BS unit and hard BT unit for PBST fibers made contribution to the lower initial modulus, higher elongation at break and better elastic recovery than those of PBT fibers. Moreover, PBST fibers were found to undergo PBT-like crystal form transition from α-form to β-form crystal structure under tension load through the measurement of WAXD. A relatively wider strain region for the crystal transition of PBST fibers also endowed them with higher elastic recoverability than PBT fibers. © 2012 Wiley Periodicals, Inc. J Appl Polym Sci 125: 2426–2432, 2012

Key words: PBST fibers; aggregation structure; tensile property; elastic property

INTRODUCTION

Biodegradable polymers have achieved great interest due to their friendliness to environment.[1–9] Among them, aliphatic–aromatic copolyester is an important series because the balance of biodegradability and physical properties can be controlled by adjusting the molar ratio of comonomers. Poly(butylene adipate-*co*-terephthalate) (PBAT, Ecoflex®) was a commercialized aliphatic–aromatic biodegradable copolymer from BASF, and its properties were reported intensively by Müller et al.[5–9]

Recently, poly(butylene succinate-*co*-terephthalate) (PBST) has received much attention[10–16] because the raw materials of 1,4-butanediol (1,4-BD) and succinic

acid (SA) can be manufactured by the method of bio-ferment.[17–19] As a melt-spinnable, biodegradable copolyester, its biodegradation, thermal, mechanical, and viscoelastic properties were investigated systematically. It is particularly noteworthy that the filaments prepared by PBST resins exhibited excellent mechanical properties investigated in our previous research.[16]

The elucidation on the relationships between aggregation structure and mechanical properties of semicrystalline polymers was the motive for extensive studies in the past years. The complexity in investigating the deformation of semicrystalline polymers arises from the presence of the two-phase structure, and the tendency existed in concentrating primarily on the transition behavior of the crystalline regions.[9] Researches on the elastic deformation characteristics showed that PBT had good elastic recovery attributed to the reversible gauche-trans-gauche conformation (α-form) to an extended phase with a trans sequence (β-form) under tension, and such crystal form transition directly affected the elastic property of PBT fibers[9,20]. However, the stretch

elastic recovery of PBST fibers, one of the most important mechanical properties evaluating their application in textiles, has never been investigated. The similar crystal transition possibly happens to PBST fibers since both of them have the same triclinic crystal structure [12]. Therefore, the purpose of this study is to investigate the aggregation structure development and mechanical properties of the as-spun PBST fibers, and then further disclose their relationships for elucidating the fiber elastic recovery mechanism.

EXPERIMENTAL

Materials and as-spun fibers preparation

PBST resins were synthesized via direct esterification and polycondensation process from the starting materials of terephthalic acid (TPA), SA and excess amount of 1,4-BD, and the detailed preparation was described elsewhere.[14] The feed molar ratio of TPA to SA was 7 : 3. PBST fibers were prepared through the melt-spinning process. The resins were dried at 110°C for 24 h before melt spinning to avoid the possible hydrolysis during extrusion process. The polymer was extruded from a 36-hole spinneret of 0.32 mm in diameter at 225°C. As-spun fibers were taken-up by a high speed winder placed at 200 cm below the spinneret at the take-up velocities of 2.0, 2.5, 3.0, 3.5, 4.0 km/min. Subsequently, the filaments were stretched with a draw ratio of 1.5. For comparison, PBT fibers supplied by Shanghai Petrochemical (China) were selected as a reference sample.

Birefringence measurements

Birefringence measurement was made with a Berek compensator mounted in a Nikon polarizing microscope. An average of 10 individual determinations was reported. The radial distribution of orientation was qualitatively evaluated through observation of the parallel polarization interference patterns using a Jena interference microscope.

WAXD measurements

A D/Max-2550 PC type of wide angle X-ray diffraction analyzer (WAXD) was used to track the crystal form transition of PBST fibers at room temperature. The power of the generator is 40 kV and 200 mA with a Nickel-filtered Cu Kα radiation (λ = 0.154 nm). The X-ray diffraction profiles were recorded at the 2θ range of 2–50° at a scan speed of 8°/min.

The values of orientation in crystalline region and crystallinity were obtained by WAXD method. For the orientation in crystalline region (Π), its value was determined via the following equation

$$\Pi = (180° - H)/180° \times 100\%$$

where H is the peak width at midheight location of intensity distribution curve for Debye diffraction ring at the equatorial line. Meanwhile, the value of crystallinity was calculated by the area ratio of crystalline peaks to all the diffraction peaks (crystalline and amorphous phase).

In the case of uniaxial oriented fiber sample, the gauge length was 10 mm. The tensile deformation was carried out by rotating the nuts at both ends. About 1600 filaments of PBST fibers, prepared at the take-up velocity of 2.0 km/min, were aligned parallel to each other at a width of 5 mm to obtain sufficient diffraction intensity. Reflections close to the meridional direction were clearly monitored by tilting the fiber bundle properly in the plane containing the X-ray beam and the fiber bundle.

Mechanical test

An electronic single yarn strength tester (Model LLy-06, Laizhou Electron instrument, China) was used to investigate the mechanical properties of PBST fibers. Sample with a gauge length of 500 mm was automatically mounted, and the tensile speed was 500 mm/min. The parameters were preset according to GB/T 14344-2003.

As to the determination of elastic property, the sample was drawn at five extension levels of 5, 10, 15, 20, and 25% at a rate of 500 mm/min. When the required extension was reached, the crosshead was stopped for 1 min to allow stress relaxation. After that, the sample was drawn back at the same rate of crosshead travel used in the extension cycle until the initial gauge length (500 mm) was reached, and then was kept for 1 min at the original place. For the test of multiple cyclic extension, repeat the first cyclic extension for required times.

RESULTS AND DISCUSSION

Aggregation structure development

The aggregation structure generally includes the orientation and crystal structures of a polymer. Birefringence was capable of revealing the orientation structure. Table I presented the birefringence values of PBST fibers melt-spun at different take-up velocities. It could be found that the birefringence values of PBST fibers increased with the take-up velocity, indicating that the higher degree of orientation was obtained by increasing the take-up velocity ranging from 2.0 to 4.0 km/min. To further elucidate the orientation structure changes of PBST fibers, the orientation in crystalline region was measured as also shown in Table I. A similar change was found

TABLE I
Aggregation Structure and Tensile Property of PBST Fibers Prepared at Different Take-Up Velocities

Take-up velocity (km/min)	Birefringence[a]	Orientation in crystalline region[b] (%)	Crystallinity[b] (%)	Breaking strength[c] (MPa)	Standard deviation of breaking strength (%)	Elongation at break[c] (%)	Standard deviation of elongation at break (%)
2.0	0.122	82.9	38.4	236.4	9.4	60.5	3.8
2.5	0.127	83.7	44.6	252.2	7.4	36.4	2.3
3.0	0.129	84.1	46.7	262.5	4.9	31.3	1.4
3.5	0.132	86.4	56.8	369.7	6.3	26.1	1.0
4.0	0.142	87.0	60.1	418.2	9.9	24.1	0.9

[a] The birefringence was measured using a polarizing microscope and a Berek compensator.
[b] The orientation in crystalline region and the crystallinity were measured by WAXD.
[c] The tensile property parameters were determined by the stress–strain curves in Figure 2.

as well. Thus, both the overall orientation and orientation in crystalline region of the fiber macromolecules increased with the take-up velocity since the fiber macromolecules were drawn by the higher tension of spinning line.

It was noted that the phenomenon that the birefringence values increased initially and then decreased with the take-up velocity, which existed in the melt-spinning of poly(trimethylene terephthalate) (PTT) fibers,[21] poly(ethylene terephthalate) (PET) and polylactide (PLA) fibers,[22] was not discovered for PBST fibers. The possible reason was that the take-up velocity for the preparation of PBST fibers was not high enough to cause the occurrence of birefringence distribution in cross-section (the well-known skin-core double structure) formed in the high-speed spun fibers.[21,22] Further experimental confirmation will be sought in future work.

It is well-known that the crystals of PBT homopolymer have two forms of α and β type, which are reversible to each other under tensile deformation and relaxation.[23–25] In the case of the prepared PBST fibers, in which soft BS unit is introduced into BT crystal lattice, interest is aroused to investigate whether the crystal structure of PBST fibers also undergoes PBT-like crystal form transition. Therefore, WAXD measurement on PBST fibers during tensile deformation was conducted. Figure 1 depicted the changes of WAXD patterns for PBST fibers at 2.0 km/min of take-up velocity during tensile deformation. With the increase of tensile deformation, peaks assigned to α-form became weaker, while the peak assigned to β-form became dominated when tensile strain was above 25%. So it was interestingly found that the crystal structure of PBST fibers also undergoes PBT-like crystal form transition under tension load. Note that, the α-form of PBT crystals totally transforms into β-form when the tensile strain is over 12%.[23] However, as to the PBST copolymer, the α-form still exists even at the tensile strain of 25% as shown in Figure 1. It can be interpreted that the lower modulus of PBST fibers

attributed to the import of soft BS unit endows them with better flexibility compared to PBT fibers as shown in Figure 3.

Tensile property

Experimentally, five contributions to the tensile deformation of polymer fibers can be distinguished[26]: (1) an elastic deformation which is an immediate and reversible response to a stress, (2) the yield deformation which is partly recoverable and (3) partly permanent, (4) a time-dependent reversible contribution, and (5) a time-dependent permanent contribution. These five deformations make complete description of the deformation of polymer fibers. Tensile property of fibers generally depends on the shape of fiber cross-section, concentration of the hard segment domains, intermolecular bonding, and the ability of soft unit to crystallize under strain.[27]

Stress–strain curves of PBST fibers prepared at various take-up velocities were plotted in Figure 2. It could be found that the initial tensile modulus and breaking strength of PBST fibers increased with increasing the take-up velocity, while elongation at
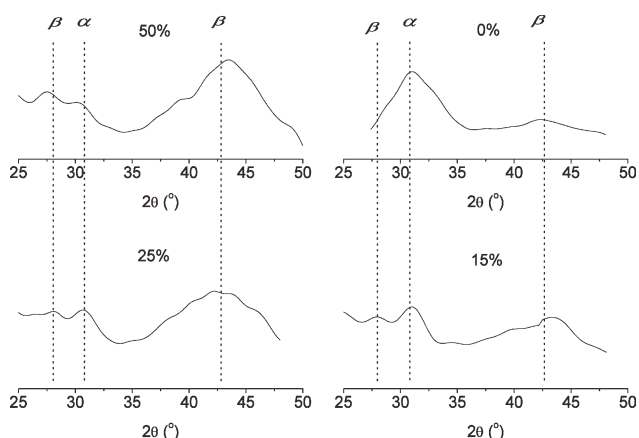

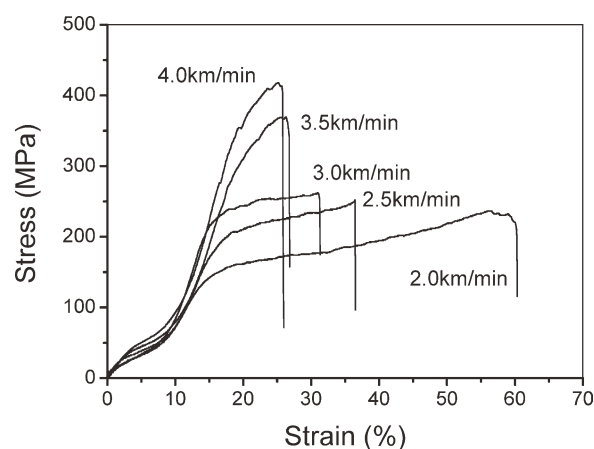Figure 1 Wide angle X-ray diffraction profiles of PBST fibers during tensile deformation.

Figure 2 Stress-strain curves of PBST fibers prepared at different take-up velocities.

break decreased. The tensile strength of PBST fibers increased significantly when the spinning speed was higher than 3.0 km/min. The changes were attributed to the increased degree of orientation, which was revealed by the above investigation of birefringence and orientation in crystalline region. Furthermore, the crystallization induced by orientation might occur when the spinning speed exceeded 3.0 km/min, and the overall increased crystallinity would also make some contribution to the improvement of tensile property as shown in Table I. With increasing the take-up velocity from 2.0 to 4.0 km/min, the increase of crystallinity was ranged from 38.4 to 60.1%, which endowed PBST fibers with elevating breaking strength from 236.4 MPa to 418.2 MPa.

To elucidate the effects of soft BS unit on the tensile property, PBT fibers were measured as a reference sample. Figure 3 plotted the stress–strain curves of PBST and PBT fibers melt-spun at 2.0 km/min. Obviously, PBST fibers presented relatively
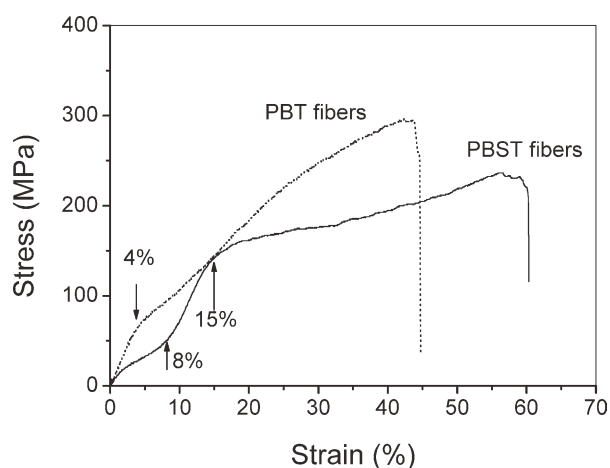
higher elongation at break and lower initial modulus, indicating that the as-prepared fibers was softer in handle than PBT fibers due to their different chemical structures. PBST fibers are composed of soft BS unit and hard BT unit, while PBT fibers are constituted only by BT unit. The higher the content of hard unit, the more rigidity the fibers display. Surprisingly, the stress–strain curve of PBST fibers was not the classic anti-s curve, but two knee points appeared respectively at the strain of 8 and 15%. Thus PBST fibers showed bilinear elasto-plastic region due to their special chemical structure composed of soft BS and hard BT unit. When the strain of PBST fibers was lower than 8%, the soft BS unit was first stretched and extended to a certain degree, while the hard BT unit began to extend as the strain exceeded 8% because the slippage of BT unit lagged due to the steric hindrance of benzene ring. Hence the slope of the tensile curve of PBST fibers at the strain threshold of 8 to 15% was higher than that of the tensile curve from 0 to 8%. When the strain of PBST fibers exceeded 15%, yield behavior occurred. So many intermolecular transverse connecting bonds are cut off and can not be returned to their original location, or new transverse connecting bonds have been reformed in a new position. If higher strain was even applied on PBST fibers, the macromolecular chains were highly oriented and even fully stretched until the rupture of PBST fibers.

Elastic property

Theoretically, the mechanical properties of fiber materials have a strong time-dependent characteristic,[28] thus strain rate should affect the elastic recovery of PBST fibers. However, the elastic recovery of PBST fibers was found to be insensitive to the strain rate at constant elongations of 5, 10, and 15% (PBST-5%, PBST-10%, PBST-15%) where the strain rate
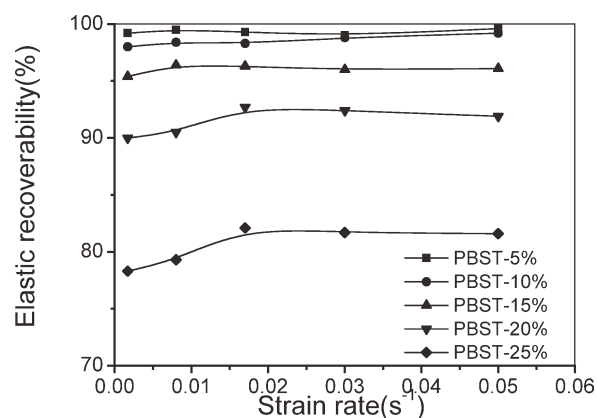

Figure 3 Stress-strain curves of PBST and PBT fibers.

Figure 4 Effects of strain rate on elastic recoverability for PBST fibers at different constant elongations.
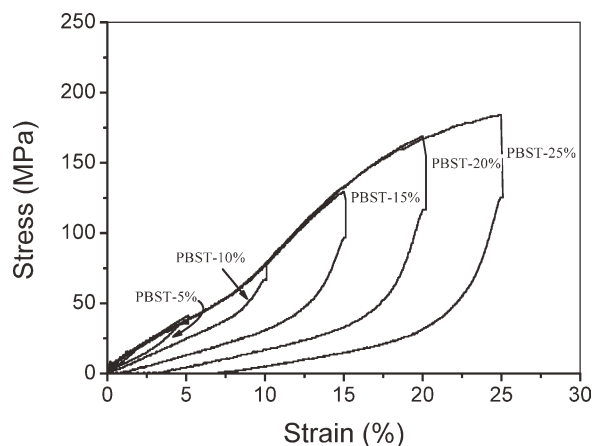
Figure 5 One-time-cyclic-stretch curves of PBST fibers stretched at different constant elongations.

ranged from 0.001/s to 0.05/s as shown in Figure 4. The result may be caused by two reasons. First, it is easy for the fiber macromolecular chains to achieve a balance under low constant elongation; second, α-form crystal of PBST fibers is the dominant crystal pattern when the elongation is lower than 15% as shown in Figure 1, which contributes to higher recoverability under various strain rates. As to the PBST fibers stretched at constant elongation of 20 and 25%, their elastic recoverability first increased and then tended to become stable. The lowest elastic recoverability was attained under the lowest strain rate since longer load time was applied on the sample, which could cause the slippage of macromolecular chains and the rearrangement of intermolecular chemical bonds, indicative of the time-dependent characteristic of PBST fibers.

Figure 5 plotted the one-time-cyclic-stretch curves of PBST fibers at different constant elongations. The notable hysteretic effect was observed in the relationship of stress to strain for the PBST fibers. This can be interpreted that the molecular chain slippage is incapable of keeping up with the alteration of the applied load due to the interaction forces existed between the macromolecules when the fibers were stretched. That is to say, the fiber deformation always lags behind the tension load, thus the stress–strain hysteresis effect appears.

TABLE II
Stretch Elastic Recoverability of PBST Fibers Prepared at Different Take-Up Velocities

Take-up velocity (km/min)	Constant elongation				
	5%	10%	15%	20%	25%
2.0	99.9	99.4	97.9	91.2	82.1
2.5	99.7	98.9	96.7	88.1	78.4
3.0	99.6	99.1	97.6	87.8	75.6
3.5	99.3	98.3	95.4	78.4	/
4.0	99.4	96.6	94.0	70.1	/

Table II summarized the stretch elastic recoverability of PBST fibers melt-spun at different take-up velocities. It could be seen that the elastic recoverability decreased with increasing the constant elongation. All the samples manifested excellent elastic recovery under the constant elongation of 5, 10, and 15%. Nevertheless, the elastic recoverability decreased distinctly when the elongation is higher than 15%, especially to the samples with take-up velocity of 3.5 and 4.0 km/min. The reason may be that both of the samples possessed higher degree of orientation before extension, and more significant slippage of macromolecular chains occurred when they were drawn to the elongation of 20% (close to their elongation at break). The high elongation can cause the distinct permanent deformation, so low elastic recoverability was found. Meanwhile, the time-dependence of stretch elastic recovery was enhanced gradually as the increasing constant elongation, because the permanent deformation caused by creep or relaxation depresses the elastic recovery as increasing the constant elongation. Therefore, the constant elongation greatly affects the stretch elastic recovery of PBST fibers.

Figure 6 showed the effects of cyclic stretch times on the stretch elastic recovery and permanent deformation of PBST fibers under different constant elongations. The elastic recoverability almost stayed unchangeable at various cyclic stretch times when the constant elongation was lower than 15%, indicating the deformation was completely reversible because α-form crystal of the fibers was the dominant crystal pattern as discussed in crystal form transition. However, as the constant elongation was higher than 15%, the elastic recoverability decreased distinctly with increasing the cyclic stretch times, and its largest descending range happened to the sample which was cyclically stretched for five times. The possible reason was that the β-form became
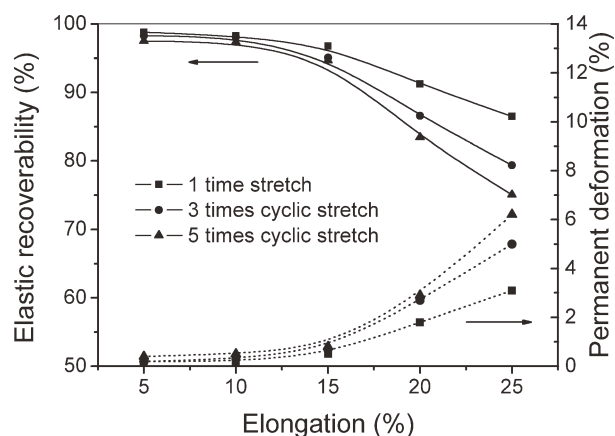

Figure 6 Effects of cyclic stretch times on the stretch elastic recovery of PBST fibers.

the prominent crystal structure which was not completely reversible.[23] Thus, the accumulated deformation that can not recover resulted in the decreasing elastic recoverability with increasing the cyclic stretch times.

Figure 7 plotted the one-time-cyclic-stretch curves of PBST and PBT fibers. ε_1 is the instantaneous elastic deformation, ε_2 is the elastic deformation that can recover in a certain time rather than immediately, and ε_3 is the permanent deformation. It could be found that PBST fibers presented relatively higher ε_1 but lower ε_3 than PBT fibers, indicative of their more excellent elastic recovery. To further explore the differences of elastic property, the changes of elastic recoverability of PBST and PBT fibers at various constant elongations were displayed in Figure 8. Obviously, PBST fibers had distinctly higher level of elastic recoverability than PBT fibers at different constant elongations, especially at higher constant elongation. The results once again proved that the former had better elastic property.

The reasons that caused the differences of elastic property of PBST and PBT fibers can be deduced as followed. PBT fibers had excellent elastic recovery under lower constant elongation (lower than 10%), but their elastic recoverability decreased significantly as the constant elongation increased because of the complete crystal transition into β-form when the constant elongation was higher than 12%.[9] Such crystal transition was not completely reversible which resulted in evident permanent deformation. However, the occurrence of crystal transition of PBST fibers was in a wider strain region which endowed the fibers with better stretch elastic recovery as discussed in the part of crystal transition. In addition, the excellent elastic property of PBST fibers may be attributed to their chemical structure consisting of hard aromatic (BT unit) and soft aliphatic units (BS unit), somewhat similar to the hard and soft segmented polyur-
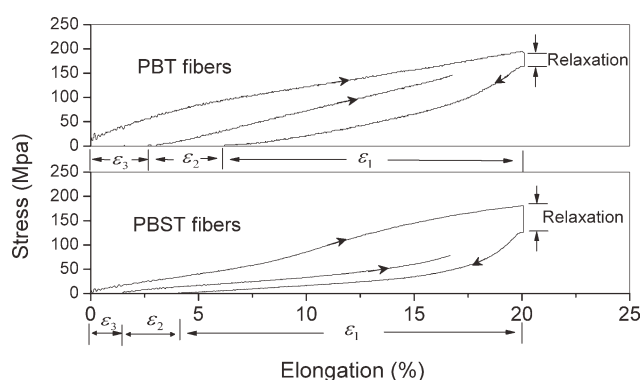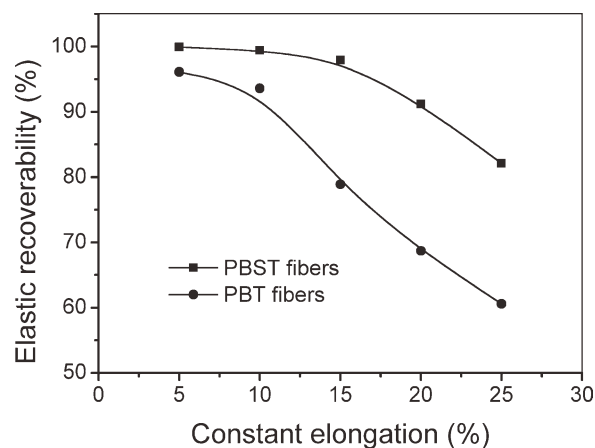

Figure 8 Changes of elastic recoverability of PBST and PBT fibers.

ethane,[29] while PBT fibers are constituted only by hard unit (BT unit).

CONCLUSIONS

Biodegradable PBST copolyester showed good spinnability in melt-spinning process with the take-up velocity from 2.0 to 4.0 km/min. High take-up velocity led to the enhancement in macromolecular orientation, crystallinity and mechanical properties of PBST fibers. The breaking strength significantly increased when the take-up velocity was higher than 3.0 km/min attributed to the occurrence of crystallization induced by orientation. PBST fibers were found to undergo PBT-like crystal transition from α-form to β-form crystal structure under tension load. The crystal transition occurred in a wider strain threshold than that of PBT fibers.

Furthermore, the tensile and cyclic stretch elastic recovery properties of PBST fibers were investigated with PBT fibers as a comparison sample. It was interesting to find that the stress–strain curve of PBST fibers was not the classic anti-s curve, but two knee points appeared respectively at the strain of 8 and 15%. The phenomenon may be caused by the fiber chemical structure which was composed of soft BS and hard BT units. The combination of soft and hard units made contribution to the lower initial modulus, higher elongation at break and better elastic recovery of PBST fibers than those of PBT fibers. The occurrence of crystal transition of PBST fibers in a wider strain region also allowed PBST fibers with higher elastic recoverability based on the comparison results of the two types of fibers.

Figure 7 The one-time-cyclic-stretch curves of PBST and PBT fibers.

References

1. Sudesh, K.; Abe, H.; Doi, Y. Prog Polym Sci 2000, 25, 1503.
2. Amass, W.; Amass, A.; Tighe, B. Polym Int 1998, 47, 89.

3. Okada, M. Prog Polym Sci 2002, 27, 87.

4. Chiellini, E.; Fernandes, E. G.; Pietrini, M.; Solaro, R. Macromol Symp 2003, 197, 45.

5. Witt, U.; Yamamoto, M.; Seeliger, U.; Müller, R. J.; Warzelhan, V. Angew Chem Int Ed 1999, 38, 1438.

6. Witt, U.; Müller, R. J.; Deckwer, W. D. Macromol Chem Phys 1996, 197, 1525.

7. Witt, U.; Müller, R. J.; Deckwer, W. D. J Environ Polym Degrad 1997, 5, 81.

8. Müller, R. J.; Kleeberg, I.; Deckwer, W. D. J Biotech 2001, 86, 87.

9. Shi, X. Q.; Ito, H.; Kikutani, T. Polymer 2005, 46, 11442.

10. Honda, N.; Taniguchi, I.; Miyamoto, M. Macromol Biosci 2003, 3, 189.

11. Nagata, M.; Goto, H.; Sakai, W.; Tsutsumi, N. Polymer 2000, 41, 4373.

12. Li, F. X.; Xu, X. J.; Hao, Q. H.; Li, Q. B.; Yu, J. Y.; Cao, A. M. J Polym Sci Part B: Polym Phys 2006, 44, 1635.

13. Li, F. X.; Xu, X. J.; Yu, J. Y.; Cao, A. M. Polym Degrad Stab 2007, 92, 1053.

14. Luo, S. L.; Li, F. X. Yu, J. Y.; Cao, A. M. J Appl Polym Sci 2010, 115, 2203.

15. Li, F. X.; Luo, S. L.; Yu, J. Y. J Polym Res 2010, 17, 279.

16. Luo, S. L.; Li, F. X.; Yu, J. Y. Int J Non-Linear Sci Num 2009, 10, 1339.

17. Stieglitz, B.; Weimer, P. Appl Environ Microbiol 1985, 49, 593.

18. Chatterjee, R.; Millard, C. S.; Clark, D. P.; Donnelly, M. I. Appl Environ Microbiol 2001, 67, 14.

19. Donnelly, M. I.; Millard, C. S.; Clark, D. P.; Chen, M. J.; Rathke, J. W. Appl Biochem Biotech 1998, 70, 187.

20. Yokouchi, M.; Sakakibara, Y.; Chatani, Y.; Tadokoro, H.; Tanaka, T.; Yoda, K. Macromolecules 1976, 9, 266.

21. Wu, G.; Li, H. W.; Wu, Y. Q.; Cuculo, J. A. Polymer 2002, 43, 4915.

22. Mezghani, K.; Spruiell, J. E. J Polym Sci Part B: Polym Phys 1998, 36, 1005.

23. Tashiro, K.; Nakai, Y.; Kabayashi, M.; Tadokoro, H. Macromolecules 1980, 13, 137.

24. Carr, P. L.; Jakeways, R.; Klein, J. L.; Ward, I. M. J Polym Sci Part B: Polym Phys 1997, 35, 2465.

25. Aljishi, R.; Taylor, P. L. Macromolecules 1988, 21, 2240.

26. Baltussen, J. J. M.; Northolt, M.G. Polymer 2003, 44, 1957.

27. Carl, B.; Wang, S. L. Macromolecules 1983, 16, 775.

28. Yi, J.; Boyce, M. C.; Lee, G. F.; Balizer, E. Polymer 2006, 47, 319.

29. Kimura, I.; Ishihara, H.; Ono, H.; Yoshihara, N.; Nomura, S.; Kawai, H. Macromolecules 1974, 7, 355.